The dynamics of the stress state in Southern California based on the geomechanical model and current seismicity: Short term earthquake prediction

V. G. Bondur[1], I. A. Garagash[2], and M. B. Gokhberg[2]

Received 20 January 2017; accepted 20 January 2017; published 3 February 2017.

The three-dimensional geomechanical model of Southern California was developed including a mountain relief, fault tectonics and internal border characteristics such as the roof of the consolidated crust and Moho surface. During the last six years on the basis of the developed geomechanical model and current seismicity is realized an approbation of technology for the estimation of possible future seismicity on a two weeks interval. All four strongest events with $M \sim 5.5-7.2$ occurred in South California during the analyzed period were prefaced by the stress anomalies in peculiar advance time of weeks-months. Inside the stress state background level investigation it was identified the feature of the large-scale interaction between two seismically active tectonic provinces of Southern California. *KEYWORDS:* Geomechanical model; stress-strain state; earthquakes.

Citation: Bondur, V. G., I. A. Garagash, and M. B. Gokhberg (2017), The dynamics of the stress state in Southern California based on the geomechanical model and current seismicity: Short term earthquake prediction, *Russ. J. Earth. Sci., 17,* ES1005, doi:10.2205/2017ES000596.

Model of the Stress-Strain State of the Earth Crust of the Southern California

In this paper we underline already a good known points, that earthquake prediction should rely on the analysis of the stress state of the Earth's crust in the studied region. Indeed, the crustal earthquakes occur as a result of the slow tectonic motions of the crust which form the geological structures and lead to the accumulation of significant elastic energy in them. The accumulated energy is released into the ambient medium due to the failure of the crustal material at the localities where the tectonic stresses reach the yield stress level.

At the same time, all the existing short-term earthquake precursors, based on various geophysical and geochemical fields, have one common significant disadvantage. The reason of the earthquake, that is the earth crust deformation, and different anomalous phenomena are related to each other via some unknown coefficient or, more precisely, via some complicated matrix. [*Bondur and Kuznetsova*, 2005; *Bondur and Pulinets*, 2012; *Bondur and Smirnov*, 2005; *Bondur and Zverev*, 2005a, 2005b, 2007; *Bondur et al.*, 2012; *Gokhberg et al.*, 1982; *Sobolev*, 1993; *Varostos et al.*, 1981].

Thus, for example, considering electromagnetic precursors, one should know mechanics-electromagnetic transformations, which should occur in different crust layers with different conductivity, porosity, permeability, fluid saturation, elasticity and so on [*Gokhberg et al.*, 1982].

The deformations observable at the Earth surface do not provide information on deep processes without knowledge of the crust geomechanical properties. The single direct source of information on the deep destructive processes is the earthquakes themselves, which happen in such places, where the local rocks are in the state close to their rigidity limits. Therefore monitoring of the stress state parameters and the rigidity may become the key point for the short-term earthquake prediction.

The earthquakes are the result of the stress state dynamics of the Earth crust and they appear in such moments and at such locations, that the rigidity limits of the rocks are achieved [*Bondur et al.*, 2016a, 2016b]. At the same time each earthquake may be considered as a new portion of the crust damage, that, in turn, causes redistribution of the stress-strain fields and affects the destructive process itself. The earthquake sequence of various rank under quasi-constant external tectonic impacts may serve as an indicator of the future seismicity progress. The tectonic impacts are well known in all seismically active areas of the Earth. The seismic networks are the most advanced global geophysical instrument. The question remains: how to use the data on the current seismicity to assess the dynamics of the stress

[1]AEROCOSMOS Research Institute for Aerospace Monitoring, Moscow, Russia
[2]Schmidt Institute of Physics of the Earth, Russian Academy of Sciences, Moscow, Russia

http://elpub.wdcb.ru/journals/rjes/doi/2017ES000596-res.html

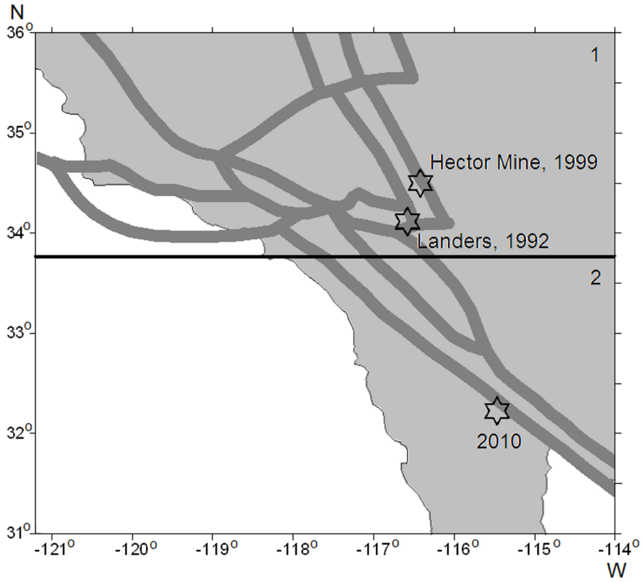

Figure 1. Map of fault tectonics of Southern California: zones 1 and 2, the northern and southern tectonic provinces, respectively.

state in order to solve the problem of the short-term earthquake prediction.

Monitoring of the current seismicity can provide data on the stress state dynamics given the Earth crust structure and external impacts are known, the latter are the basis for the geomechanical modeling. The model includes the faults tectonics, which is a stationary damage function, boundaries and elastic properties of the crust. The stress state is induced by external tectonic and gravitational impacts. Geomechanical model allows to construct 3D image of the stress state of the seismically active zone. The current seismicity is introduced into the model as an additive to the stationary damage, thus introducing the time dependence. The future seismicity forecast may be implemented by means of analysis of 4D stress state distribution. Locations of potential seismic risk are recognized as zones of anomalous stress state and proximity of the crust to the rigidity limits.

Such a monitoring take place from 2009 on South California region on the base of geomechanical model and local current seismicity [*Bondur et al.*, 2016a, 2016b]. At first the calculation of the background level strain-stress parameters behaviour will be done by seismicity less $M \sim 5.5$, where the regular big scale interaction of the tectonic provinces was detected. The tectonic map of Southern California divided by a horizontal line into two zones is shown in Figure 1.

The tectonically active area located between 34–36°N (zone 1) is formed by the junction of the longitudinal San Andreas Fault and the latitudinal Garlock and Mount faults. This causes a relatively mosaic pattern of the faulting crust. The greatest seismic events occurred here in 1992 and 1998 with $M = 7.1$ and 7.0 close to the settlement of Landers and to the town of Hector Mine, respectively. A tectonically active area south of 34.0°N (zone 2) is characterized by a relatively simple two dimensional structure, which is formed by the south end of the San Andreas Fault, and was host to a large seismic cluster with magnitude $M = 7.2$ in 2010.

The tectonic interaction of these provinces is revealed on the basis of analysis of the dynamics of the stress state for all of Southern California over 2013–2015 using a detailed geomechanical model and data on the local seismicity [*Bondur et al.*, 2007, 2010, 2016a, 2016b]. The model contains mountainous relief, the top of the lower crust, and the Mohorovicic surface and takes into account the distribution of faults (Figure 2). The fault is a tectonic zone with a complex internal structure. The fault affects the area along three directions in its vicinity [*Bondur and Zverev*, 2005a, 2005b, 2007; *Lobatskaya*, 1987]. The density of the distribution of faults (or the degree of damage to the medium) was calculated using the results of processing of space images [*Bondur and Zverev*, 2005a, 2005b, 2007]. The degree of damage to the medium is characterized by a function of heterogeneity, which is 1 on the fault axis and 0 outside the zone of its influence and which is approximated by the spline function.

All the mechanical parameters are given as follows

$$\Pi(x_s) = \Pi^0[1 - \kappa g(x_s)] \quad (1)$$

where Π^0 is the homogenous initial value of the parameter for the unbroken plate and κ is the parameter of smallness.

As a result of seismic processes, the function of heterogeneity $g(x_s)$ changes and gets the increment $\Delta g(x_s)$. To find $\Delta g(x_s)$, as well as function $g(x_s)$, the degree of damage was estimated as the increase in the length of the lineaments. It was considered that this results in the formation of a fault, the length of which (cm) is determined by the formula [*Kasahara*, 1985]

$$\log L = 3.2 + 0.5M \quad (2)$$

In the case of an earthquake with magnitude $M = 4$, the length of the forming fault is 1600 m. First, we calculated the initial stress state of the model under the influence of forces of dead weight and horizontal tectonic movements. Further, we calculated the changes in the stress state of the crust relative to the evolution of the seismic process. Each earthquake creates elemental damage, which, taking into account (2), was included into the model of the crust. A seismic flow of rocks is an assemblage of a number of seismic events [*Riznichenko*, 1985]. The dynamics of the stress state was calculated through the fortnightly periods using 3 month seismic data of 3000–4000 events, which occur mostly in the distinguished layer of the upper crust at a depth of 3.5–10.5 km. The function of strength characterizes the stress state of the crust and allows estimation how much the stress state is close to the strength limit

$$F = c\cos\varphi - \left(\frac{\sigma_1 - \sigma_3}{2} + \frac{\sigma_1 + \sigma_3}{2}\sin\varphi\right)$$

The lower the parameter F, the closer the state to the strength limit. As a result of the seismic tectonic flow, the major stresses get increments and the stress state either approaches the strength limit or moves away from it by a value of

$$D = \frac{\Delta\sigma_1 - \Delta\sigma_3}{2} + \frac{\Delta\sigma_1 + \Delta\sigma_3}{2}\sin\varphi \quad (3)$$

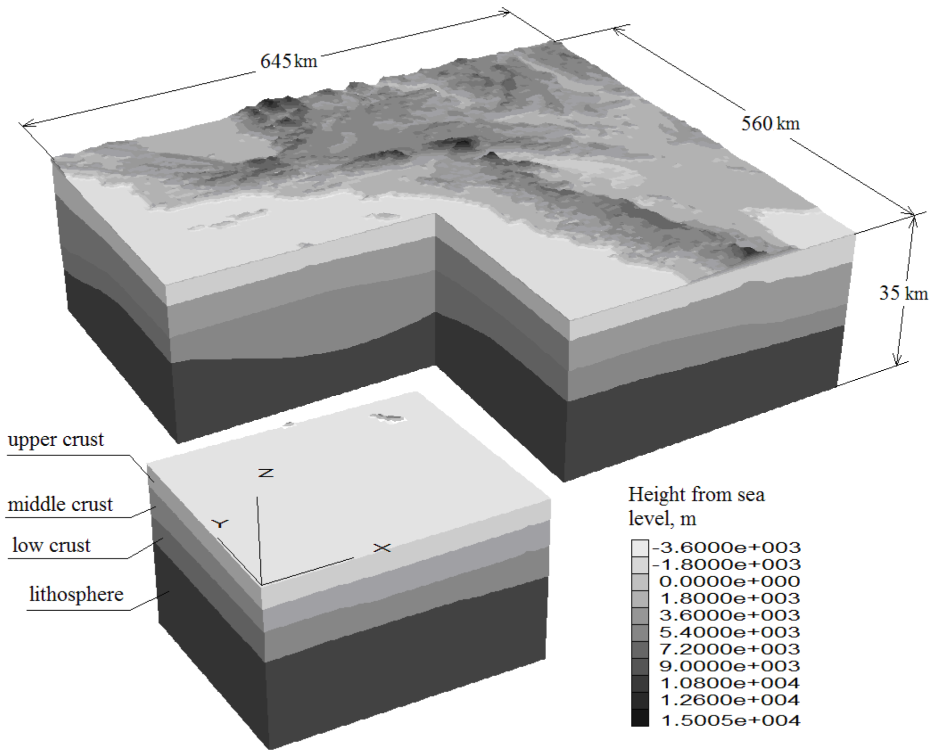

Figure 2. Model of the crust of Southern California.

where φ is the angle of friction, c is the cohesion, σ_1 and σ_3 are the major stresses, $\Delta\sigma_1$ and $\Delta\sigma_3$ are the stress increment.

Observation of parameter D allows us to forecast the increase in seismic activity in the region and to distinguish the areas with possible earthquakes, which are characterized by satisfactory convergence in the given period [*Bondur et al.*, 2014].

Large Scale Interaction Between Two Seismically Active Tectonic Provinces of Southern California

The increments of intensity of shear deformations are another informative parameter, which are calculated for the entire region with a detail of 5×5 km for each layer of the upper and middle crust

$$\Gamma = \frac{2}{3}\times$$

$$\sqrt{(\varepsilon_{11}-\varepsilon_{22})^2+(\varepsilon_{22}-\varepsilon_{33})^2+(\varepsilon_{33}-\varepsilon_{11})^2+6(\varepsilon_{12}^2+\varepsilon_{23}^2+\varepsilon_{13}^2)}$$

where are the components of the deformation tensor. The maximum deformations of the order of 10^{-4} were observed in the second layer of the upper crust, which hosts almost all seismicity.

It should be noted that the order of deformation is not calibrated.

The increments of maximum shear deformations and parameter D were observed in the entire territory studied (Figure 1). Figure 3 shows the temporal series of increments of the maximum values of intensity of shear deformation on a fortnightly period (a); a plot of the corresponding latitudes (b), which allows determination of the occurrence of areas with maximum deformations to the northern or southern provinces (zones 1 and 2); and the temporal series of increments of the strength parameter in the southern province (c). It follows from the comparison of the temporal series (Figure 3) that the maximum increments of shear deformations were observed in the north of the territory (zone 1) and were at the level of relatively high values of the order of $(2-4)\times 10^{-4}$, whereas increments of the normalized values of the parameter of the strength of rocks D were lower than the background values (0.4–0.5) in the southern province (zone 2). At the same time, when the increments of intensity of shear deformations in the north (zone 1) decrease below, the crustal rocks in the south (zone 2) approach the strength limit. In other words, when shear deformations in the upper crust at depths of 3.5–10.0 km increase in the northern province (the displacements in the San Andreas Fault area are directed from the south to the north), the stress state in the southern province is at the background level. The pause in the flow of the rocks in the northern areas (as if a barrier is formed) results in accumulation of stress even for relatively weakly variable deformations in the southern end of the San Andreas Fault. This is manifested

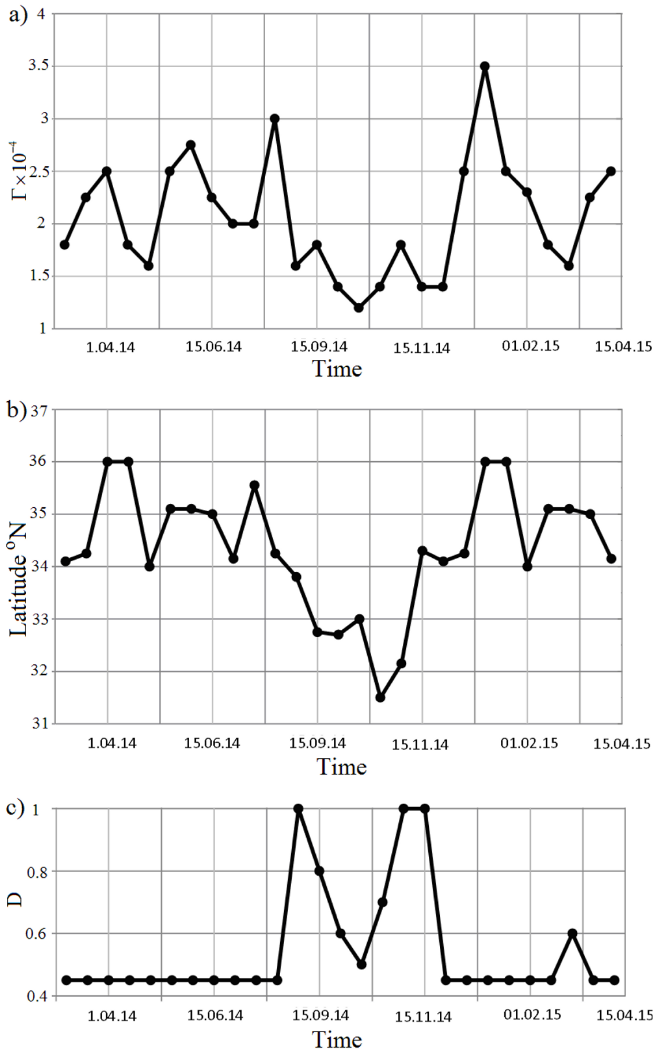

Figure 3. Temporal series characterizing the deformation processes of the studied seismically dangerous territory from March 2014 to April 2015: (a) maximum intensity of shear deformations for the entire territory; (b) plot of latitudes for the areas with maximum deformations; (c) parameter (closeness of the crustal rocks to the strength limit) in zone 2.

in the approach of rocks to the strength limit. The period in which the crustal rocks in the southern province occur in a stress state close to the strength limit is 3.5 months, and the transitional period is 0.5 month.

This indicates a relatively fast jump change in the stress state over ~ 0.5 month under the duration of a regime of one month to one year that allows us to estimate quantitatively the rheological properties of the crust at the macrolevel.

Such a relatively fast change in the stress state of the crust of the seismically active region opens new prerequisites for the short term prediction of earthquakes at a typical period from a week to a month.

The feature revealed is consistent with ideas on the dynamics of the stress state of the crust in a system of faults with a significantly distinct structure of the areas. It was obtained experimentally for the first time as a result of monitoring of the geomechanical model behavior using the data on the current local seismicity.

It is important to note that the calculated values of shear deformation are given for the upper crust deeper than 5 km, where the major flow of the rocks is related to the local seismicity and caused the dynamics of the stress state of the entire region. Closer to the surface and on the surface, the deformations are significantly lower and do not cause variations in the parameters of the stress state, which are indicative of evolution of the seismic processes. At the same time, the instrumental observations for the displacements of the crust provide, as a rule, information on the surface deformations. The latter provides for a significant advantage of the calculations on the basis of instrumental seismic observations in the framework of the geomechanical model reviewed. It should also be noted that the calculated values of increments of the model parameters depend on the chosen value of the coefficient of smallness κ in formula (1). This influences only the amplitudes of values but not the principles of their distribution. Further improvement of the model will allow calibration of the coefficient κ. The period studied is characterized by weak background seismicity for this region with $M < 5.5$. Our result, however, is more important for understanding the dynamics of the tectonic processes of this region and prediction of stronger seismicity. In fact, the background increments of shear deformations in the southern province are less $(1.0 - 1.5) \times 10^{-4}$. These deformations lead to a notable increase in the background values of the parameter D, which characterizes the stress state of the crust. It is evident that stronger deformations in the southern province may result in a state of critical stress, which could cause a significant earthquake. Thus, continuous monitoring of variations in shear deformations along with parameter D in the framework of this model may enhance significantly the solution of the problem of the short term prediction of strong seismic events for periods from a week to a month.

What kind of the tectonic province interaction take place before the largest for last time seismic cluster 2009–2010 with $M = 5.5 - 7.2$?

On the Figure 4a and Figure 4b the maximal shear strain variations and parameter D are done.

As we can see from the Figure 4a, the shear deformation variation exceed the background level around 3 times for one month before the largest of the last time in California event with $M = 7.2$, which occur 04.04.2010 with coordinate 32.26°N, 115.29°W and practically take place along all south part of San Andreas fault with the latitudes 32–36°N.

From the Figure 4b we can see: the amplitude of parameter D begin to exceed background level ($D = 3 \times 10^4$ Pa) around 3.5 month before the event and reach the value ($D = 8.7 \times 10^4$ Pa).

We can see also the strong oscillations with the amplitude around $D = 5 \times 10^4$ Pa and period $T \sim 1.5 - 3.0$ month.

Thus, unlike from the background situation of the tectonic province interaction the shear strain essentially increase on the period of the large seismic event preparation as in the south as in the north provinces. This lead to the periodical accumulation of the elastic energy and maximal for all time

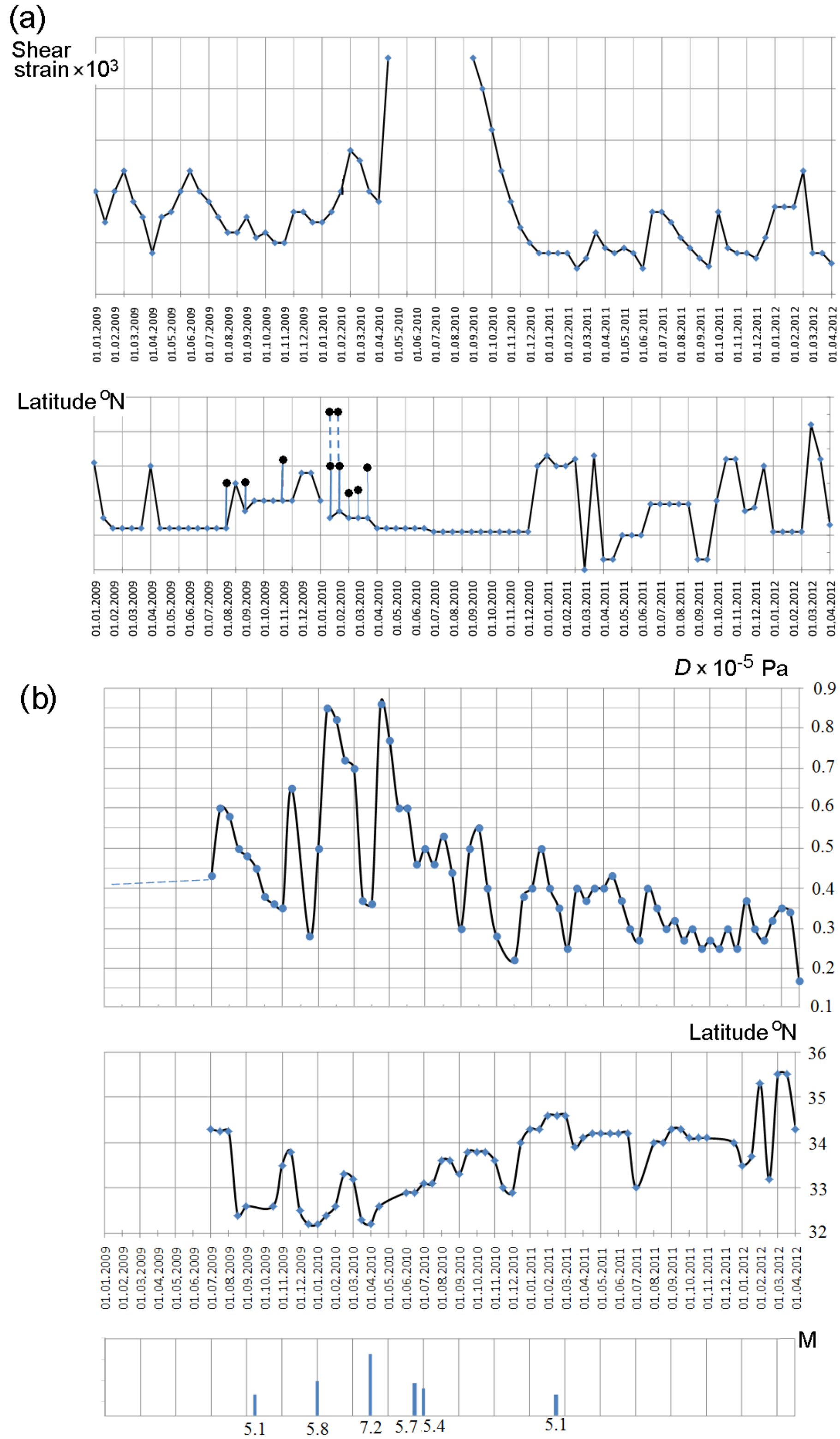

Figure 4. a) graphic above: the shear deformations intensity maximum by calculation on the depth 3.5–10 km, (layer 2 of the upper Earth crust in the model, where all seismicity in general take place), vertical line show the simultaneous appearance of the larger deformation to the north along the fault from the future epicenter $M = 7.2$, graphic below: the latitudes on San Andreas fault with the shear deformation maximums, vertical lines show the place with simultaneous appearance of deformation; b) graphic above: the parameter D maximum variation – approaching the earth crust to the strength limit, graphic below: the latitudes on San Andreas, where D maximum take place. The calculations rely to 1-th and 15-th each month.

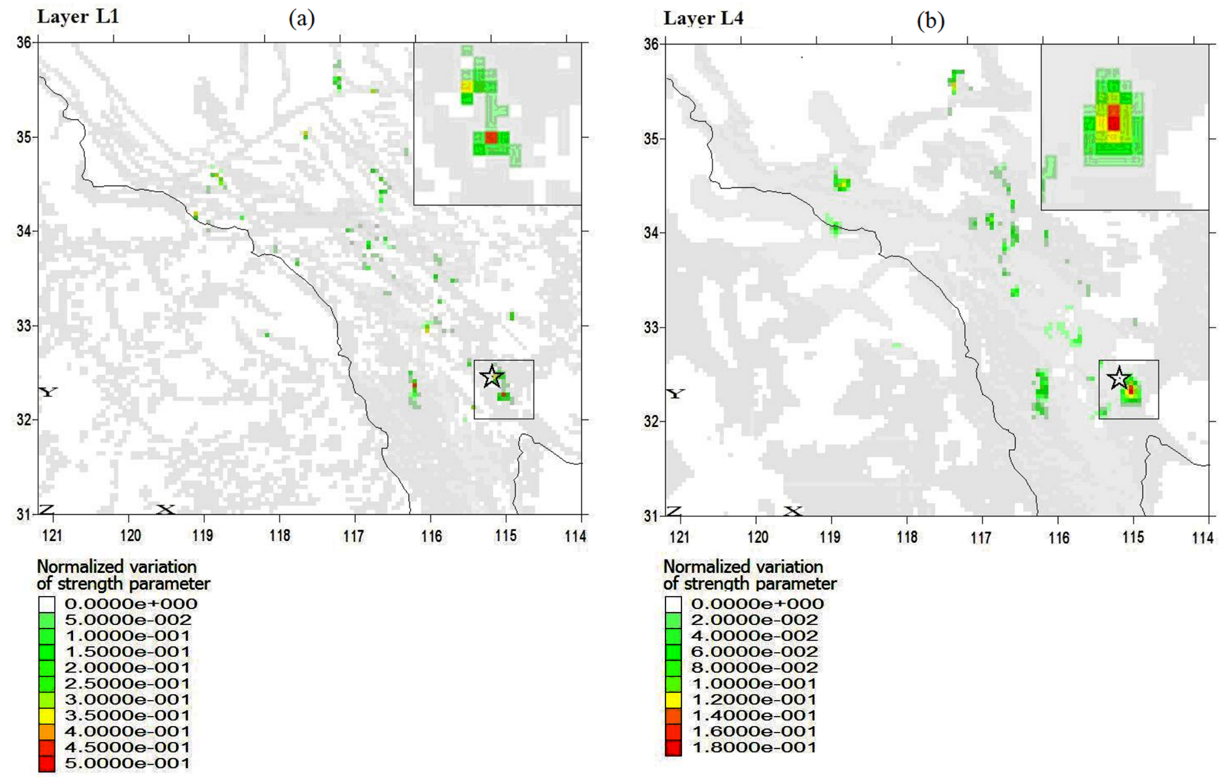

Figure 5. The normalized distribution of the strength parameter D describing the closeness of the stress state to the yield stress as of December 15, 2009: (a) in the layer 1 (upper crust); (b) in the layer 4 (middle crust).

(2009–2016) approach the upper crust rocks to their strength limit relatively to the "stress-strain" dependence.

Further, the space-time distributions of the stress state parameters (on the parameter D example) for all large events of the cluster 2009–2010 are presented.

In the modeling of the seismic process, it should be taken into account that the shear strain on the faults are controlled by the forces of dry friction in accordance with the Mohr–Coulomb yield criterion. Thus, the system of the blocks initially undergoes elastic deformation; then, once the yield condition is satisfied, the system comes into motion. As a result, the angle of internal friction drops stepwise to a certain minimum value, and the new equilibrium is established under the lower stress level. In this case, the effective mechanical properties of the medium are changed in the vicinity of the seismic event. This leads to the redistribution of the stresses in the crust and, eventually, prepares a new strong earthquake.

Evolution of the Stress State Before Strong Earthquakes

The distributions of seismic energy released during a three month interval starting from 2009 are used as the input data for the calculations. At each step, the time window is shifted by 15 days. When the stresses are calculated on the previous and subsequent time intervals, the difference between the two stress states is determined, and the ongoing changes are estimated from this difference. The variations in the distributions of the maximum shear stresses, accumulated elastic energy, and closeness of the stress state to the yield limit are constructed. Only those crustal segments are considered on which the parameters are positive (the subsequent value is larger than the previous one). Damage accumulation is accompanied by damage healing. Therefore, the model includes the function which describes the gradual decline of the effects of the accumulated damage. The healing rate is a rather uncertain parameter. It is assumed that at each time step, the previous accumulated damage diminishes by one-eighth of the value. The calculated stress distribution provides an idea of how close the crustal state is to the yield stress. This can be seen from the distribution of the strength parameter D (see formula (3)) which characterizes the closeness of the stress state to the strength surface. The smaller values of D correspond to the stress state farther from the yield stress. The 3D distribution of the new parameter (the closeness of the crustal segments to the yield stress), which is calculated every two weeks, specifies the locations of the future earthquakes that are likely (with a reasonable probability) to occur during a given time interval.

In order to exemplify the application of the described method, we cite the calculated changes in the strength of the Earth's crust prior to the earthquake with magnitude

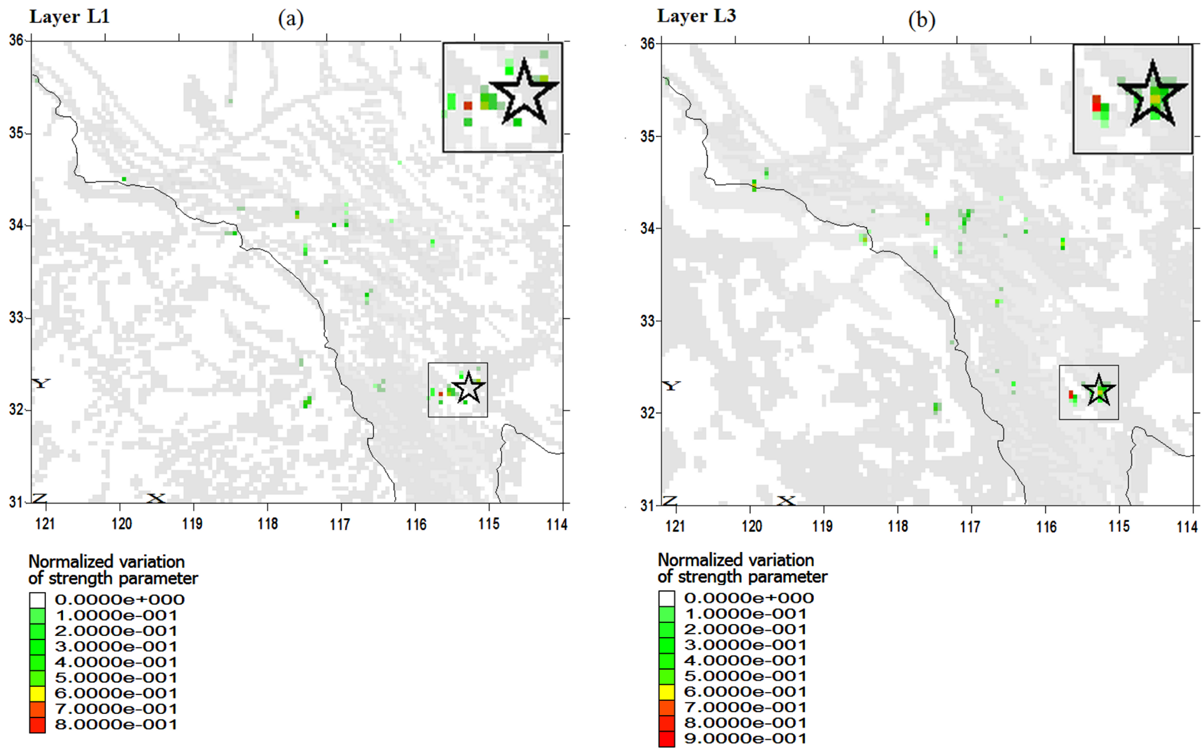

Figure 6. The normalized distribution of the strength parameter D describing the closeness of the stress state to the yield stress as of April 4, 2010: (a) in layer 1 (upper crust); (b) in layer 3 (middle crust).

5.9 which occurred at 1848 UT on December 30, 2009 in Baja California, Mexico at a depth of 7 km. The epicenter of this event was at 32.464°N and 115.189°W. Immediately before the main shock, two foreshocks with magnitudes 3.53 and 2.43 occurred at 1754 and 1757 UT in the epicenter of the main shock. The hypocenters of these foreshocks were located at a depth of 15 and 6 km, respectively. The main event was followed by two aftershocks. The first aftershock with a magnitude of 4.9 and the hypocenter at 3.5 km occurred at 1853 UT. The second aftershock occurred at 1904 UT; it had a magnitude of 3.4 and a hypocenter depth of 35 km. The analysis of the stress state maps as for the second half of December 2009 shows that the earthquake hit the location where the stress state approached the yield stress in the upper layer $L1$ at a depth of about 3 km (Figure 5a) and in the layer $L4$ (Figure 5b, middle crust at a depth ranging from 20 to 35 km). Thus, it can be concluded that the foreshocks initially hit the upper layer and middle crust and it was only after this that the main rupture ran between them at a depth of ~ 6 km. Next, the aftershocks again occurred in the upper layer and middle crust in the areas where the strength of the rocks was rather low.

Figure 6 shows the state of the strength parameter D in layers 1 and 3 on April 1, 2010, before the strong earthquake with a magnitude of 7.2, which occurred on April 4, 2010. The spatial migration of the sources of the stressed state, according to the variations in the strength parameter D within ~ 3 months before the event, is illustrated in Figure 7. It can be seen that the anomaly appears east of the future epicenter at a distance of $R \sim 20$ km. Then the anomaly migrates closer to the epicenter ($R \sim 10$ km) and simultaneously arises northwest of the epicenter, where it follows the San-Andreas fault ($R \sim 30$ km). Next, the anomaly shifts north to $R \sim 50$ km, after which the anomalous area progressively moves towards the epicenter of the future event with $M = 7.2$. Figure 7 shows that the anomalous gradients of D appear in the layer 2 around 50–35 days before the earthquake. This zone of anomalous gradients emerges 20 km northwest of the epicenter and stretches along the San-Andreas fault. As of April 1, 2009, i.e., three days prior to the earthquake, this anomaly in the layer 2 disappears and moved to the layer 3 in the immediate proximity of the epicenter and simultaneously around 30 km west. At the 10 days after event, the area of the maximum values migrates northwest along the San-Andreas Fault to a distance of $R \sim 70$ km and farther towards the epicenters of the future events of June 15, 2010 ($M = 5.8$) and July 7, 2010 ($M = 5.5$).

An example of the evolution of the strength parameter D in layer 4 (middle crust) during the interval from May 15, 2010 to September 1, 2010, which accommodates two earthquakes, is shown in Figure 8. One earthquake with magnitude 5.8 occurred on June 15, 2010 at 32.7°N, 115.92°W. The other event with magnitude 5.5 occurred on July 7, 2010 at 33.42°N, 116.49°W. The figure shows that before the earthquake of June 15, 2010, a crustal segment within layer 4 approached the yield stress (Figure 8a–Figure 8c). Closer to the event of July 7, 2010, the second crustal segment with

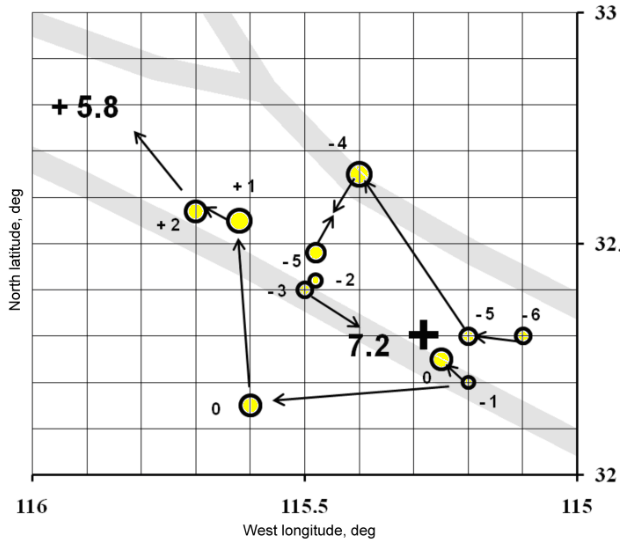

N	Date 2010	*D*	Layer N
-6	1.01	0.65	3
-5	15.01	0.7	3
-5	15.01	0.8	3
-4	1.02	1	3
-3	15.02	0.65	2
-2	1.03	0.55	2
-1	15.03	0.5	3
0	1.04	0.9	3
+1	15.04	1	1
+2	1.05	0.9	3

Figure 7. The migration of the maxima in the variations of the stress state gradient (in terms of parameter D) in the epicentral area of the earthquake with $M = 7.2$ of April 4, 2010 during the interval from January 1 to May 1, 2010. The gray lines show the main faults. The values in the table are indicated with a 2-week interval. The minus sign indicates the time before the event, and the plus sign indicates the time after the event.

a lower strength started to be formed (Figure 8c and Figure 8d), and it is this segment above which the seismic shock occurred (Figure 8e and Figure 8f). Simultaneously, the first crustal segment after the earthquake withdrew from the yield stress. By September 1, 2010 (Figure 8f), the situation in the region stabilized. During the interval from 2009 to 2011, the studied region experienced four significant earthquakes with $M = 5.5 - 7.2$. All these events were preceded by the emergence of the maximum in the strength parameter D (the closeness of the crustal segments to the yield stress) within a radius of $R < 50$ km of the future epicenter and within the time $\Delta t = 0.5 - 3$ months before the event. This is illustrated by Figure 5–Figure 8.

The situation on the earthquake preparation time show that the anomaly regions when the crust rocks approached to the strength limit move as around future epicenter as with the depth between the upper and middle crust layers. The velocities of the such movements is enough high and reached around tens kilometers per month, that probably give a key points to the better understanding of the earthquake origin processes.

It is necessary to underline, that in the time of all seismic cluster 2009–2010 preparation the Earth crust rocks in epicentral region are approached maximal to the strength limit on the stress-strain curve rely with D parameter in the model, and absolute value of the parameter reached its maximum for all 7-th years period $D = 8.7 \times 10^4$ Pa by stable background level $D = 3 \times 10^4$ Pa (Figure 4). More over, the shear strain exceed in 3 times the background level, which remain on the level 2×10^{-4} Pa for all monitoring period by seismicity less $M < 5.5$. This point permit to conclude, that in this model calculations the possibility to the "false alarm" appearance do not exist.

Conclusions

The source mechanics and earthquake prediction studies in Southern California have been conducted for a long time. Among these studies we note the theoretical works [*Ben-Zion*, 2001; *Ben-Zion and Rice*, 1995; *Rice*, 1983; *Sobolev*, 1993]. In parallel, earthquake forecasting methods have been developed [*Bondur and Zverev*, 2005a, 2005b, *Gokhberg et al.*, 1995; *Jordan*, 2006; *Keilis-Borok and Soloviev*, 2010; *Keilis-Borok et al.*, 2004; *Molchan and Keilis-Borok*, 2008].

Our analysis shows that the construction of 3D geomechanical models enables the geological, geophysical,and seismological data to be jointly used for monitoring the stress state variations which occur during the seismic process. This makes it possible to localize the regions which are likely to experience the enhancement of seismic activity in the future. In the present paper, we demonstrate one of the probable schemes of monitoring the future seismicity in the interval of days–weeks–months in advance of the event. The continuous analysis of the stress state of the rocks was conducted during four years, from 2009 to 2013. Monitoring is based on the study of the dynamics of the crustal stress state in the realistic geomechanical model with regular allowance for the current seismicity. Each new earthquake starting from magnitude $M \sim 1$ according to the USGS catalog was considered as a new defect in the Earth's crust, which has a certain size and leads to the rearrangement of the stress state. The entire calculation was based on a single function–the crustal damage function, which was updated every 0.5 months. As a result, every 0.5 months, the areas with the maximum values of the stress state parameters (elastic energy density, tangential stresses, and the closeness of crustal segments to

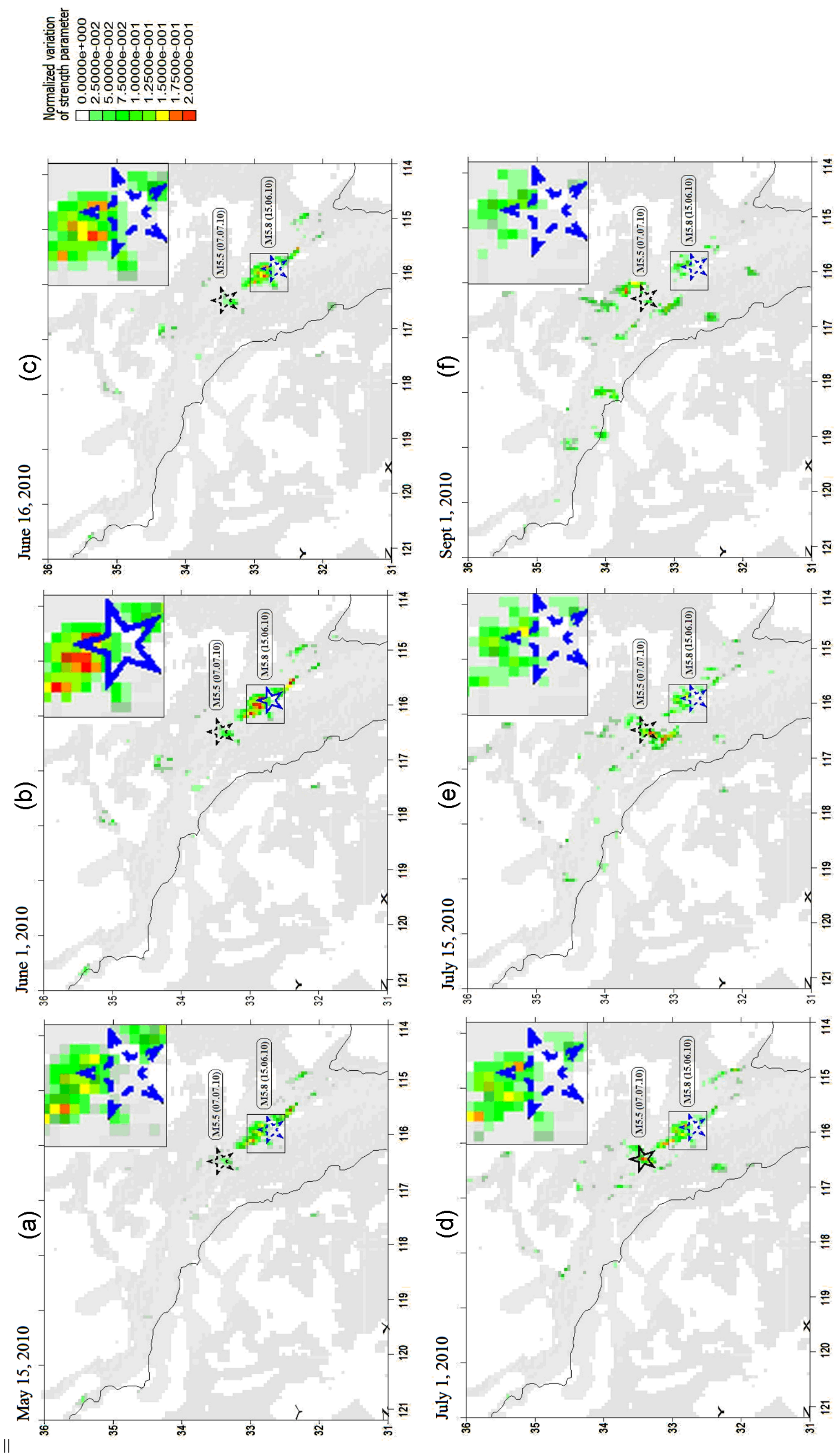

Figure 8. The evolution of the distribution of the strength parameter D in layer 4 (middle crust) from May 15 to September 1, 2010.

the yield stress) were identified in the layers of the upper and, partly, middle crust. All these parameters give nearly the same patterns of the spatial and time distributions. In this work, we present the illustrations for the normalized strength parameter D which describes the closeness of the rocks to the yield stress. As can be seen from the presented graphs, all the four most significant earthquakes with $M \sim 5.5-7.2$, which occurred during the studied time interval in Southern California, were preceded by the anomalies in the strength parameter D, which appeared within the characteristic times of a few weeks to months before the event at a distance of 10–50 km of the future epicenter. After the earthquake, the source of the stressed state disappeared.

As of now, all the calculated parameters of the stress state within the southern termination of the San-Andreas Fault, where there was previously a cluster of strong seismicity, are within their background values. We note that the present, reasonably good results on applying the described method are obtained on a rather simple, segment of the San Andreas Fault that is close to linear. North of this segment, in the junction zone of the San Andreas and Garlock faults, the pattern is, to a considerable degree, mosaic and its analysis lies beyond the scope of the present work.

In conclusion, we note that the 7-year experience of the works on monitoring the stress state before the strong earthquakes in Southern California can be used and further developed both within the studied territory and in other seismically hazardous regions.

Acknowledgments. This work carried out in AEROCOSMOS was supported by the Russian Science Foundation, project no. 16-17-00139.

References

Ben-Zion, Y. (2001), Dynamic rupture in recent models of earthquake faults, *J. Mech. Phys. Solids*, *49,* 2209–2244, doi:10.1016/S0022-5096(01)00036-9

Ben-Zion, Y., J. R. Rice (1995), Slip patterns and earthquake populations along different classes of faults in elastic solids, *J. Geophys. Res.*, *100,* 12959–12983, doi:10.1029/94JB03037

Bondur, V., L. Kuznetsova (2005), Satellite monitoring of seismic hazard area geodynamics using the method of lineament analysis, *Proc. 31st Int. Symp. on Remote Sensing of Environment* p. 376–379, ISRSE, St. Petersburg.

Bondur, V. G., S. A. Pulinets (2012), Effect of mesoscale atmospheric vortex processes on the upper atmosphere and ionosphere of the Earth, *Izvestiya, Atmospheric and Oceanic Physics*, *48,* No. 9, 871–878, doi:10.1134/S0001433812090034

Bondur, V. G., V. M. Smirnov (2005), Method of seismic danger area monitoring according to ionosphere variations, registered by satellite variation systems, *Doklady Akademii Nauk*, *402,* No. 5, 675–679.

Bondur, V. G., A. T. Zverev (2005a), A method of earthquake forecast based on the lineament analysis of satellite images, *Doklady Earth Sciences*, *402,* No. 4, 561–567.

Bondur, V. G., A. T. Zverev (2005b), A method of earthquake forecast based on the lineament dynamics analysis using satellite imagery, *Issledovanie Zemli iz Kosmosa*, No. 3, 37–52. (in Russian)

Bondur, V. G., A. T. Zverev (2007), Lineament system formation mechanisms registered in space images during the monitoring of seismic danger areas, *Issledovanie Zemli iz Kosmosa*, No. 1, 47–56. (in Russian)

Bondur, V. G., I. A. Garagash, M. B. Gokhberg (2016a), Large scale interaction of seismically active tectonic provinces: the example of Southern California, *Dokl. Earth Sc.*, *466,* 183–186, doi:10.1134/S1028334X16020100

Bondur, V. G., I. A. Garagash, M. B. Gokhberg, V. M. Lapshin, Yu. V. Nechaev (2010), Connection between variations of the stress-strain state of the Earth's crust and seismic activity: the example of Southern California, *Dokl. Earth Sc.*, *430,* 147–150, doi:10.1134/s1028334x10010320

Bondur, V. G., I. A. Garagash, M. B. Gokhberg, V. M. Lapshin, Yu. V. Nechaev, G. M. Steblov, S. L. Shalimov (2007), Geomechanical models and ionospheric variations related to strongest earthquakes and weak influence of atmospheric pressure gradients, *Dokl. Earth Sc.*, *414,* No. 4, 666–669, doi:10.1134/S1028334X07040381

Bondur, V. G., I. A. Garagash, M. B. Gokhberg, M. V. Rodkin (2016b), The Evolution of the Stress State in Southern California Based on the Geomechanical Model and Current Seismicity, *Izv., Phys. Solid Earth*, *52,* No. 1, 117–128, doi:10.1134/S1069351316010043

Bondur, V., I. Garagash, M. Gokhberg, G. Steblov (2014), Monitoring of the stress state variations of the Southern California for the purpose of earthquake prediction, *Proc. Fall Meeting of American Geophysical Union, San Francisco, Dec. 15–19, 2014* p. NH21C-05, AGU, Washington. (https://agu.confex.com/agu/fm14/webprogram/Paper17176.html)

Bondur, V. G., A. T. Zverev, E. V. Gaponova (2012), Geodynamic features of seismic areas of Russia, based on lineament analysis, *Current Problems in Remote Sensing of the Earth From Space*, *9,* No. 4, 213–222.

Gokhberg, M. B., V. A. Morgounov, T. Yoshino, I. Tomizawa (1982), Experimental measurements of electromagnetic emissions possibly related to earthquakes in Japan, *J. Geophys. Res.*, *87,* No. B9, 7824–7828, doi:10.1029/JB087iB09p07824

Gokhberg, M. B., V. A. Morgounov, O. A. Pokhotelov (1995), *Earthquake Prediction: Seismo-electromagnetic phenomena*, 191 pp., Gordon and Breach Publishers, Australia, United Kingdom.

Jordan, T. H. (2006), Earthquake predictability, brick by brick, *Seismological Research Letters*, *77,* No. 1, 3–6.

Kasahara, K. (1985), *Earthquakes Mechanics*, Cambridge Univ. Press, Cambridge, England.

Keilis-Borok, V., P. Shebalin, A. Gabrielov, D. Turcotte (2004), Reverse tracing of short-term earthquake precursors, *Physics of the Earth and Planetary Interiors*, *145,* 75–85, doi:10.1016/j.pepi.2004.02.010

Keilis-Borok, V. I., A. A. Soloviev (2010), Variations of trends of indicators describing complex systems: Change of scaling precursory to extreme events, *Chaos: An Interdisciplinary Journal of Nonlinear Science*, *20,* No. 3, doi:10.1063/1.3463438

Lobatskaya, R. M. (1987), *Structure Zoning of Crust Fractures*, Nedra, Moscow. (in Russian)

Molchan, G., V. Keilis-Borok (2008), Earthquake prediction: Probabilistic aspect, *Geophys. J. Int.*, *173,* 1012–1017, doi:10.1111/j.1365-246X.2008.03785.x

Rice, J. (1983), Constitutive relations for fault slip and earthquake instabilities, *Pure Appl. Geophys.*, *121,* No. 2, 187–219, doi:10.1007/BF02590135

Riznichenko, Yu. V. (1985), *Problems of Seismology. Selected Works*, Nauka, Moscow. (in Russian)

Sobolev, G. A. (1993), *Fundamental of Earthquake Prediction*, 313 pp., Nauka, Moscow. (in Russian)

Varostos, P., K. Alexopoulos, K. Nomicos (1981), Seismic electric currents, *Proceedings of the Academy of Athens*, No. 56, 277–286.

V. G. Bondur, AEROCOSMOS Research Institute for Aerospace Monitoring, Gorokhovskii per. 4, Moscow, 105064 Russia. (vgbondur@aerocosmos.info)

I. A. Garagash and M. B. Gokhberg, Schmidt Institute of Physics of the Earth, Russian Academy of Sciences, ul. Bol'shaya Gruzinskaya 10, Moscow, 123995 Russia. (garagash@mail.ru)